Sequential Monte Carlo filter for state estimation of LiFePO$_4$ batteries based on an online updated model

Jiahao Li*, Joaquin Klee Barillas, Clemens Guenther, Michael A. Danzer

Zentrum für Sonnenenergie- und Wasserstoff-Forschung Baden-Württemberg, Lise-Meitner-Str. 24, 89081 Ulm, Germany

HIGHLIGHTS

- A novel framework for state estimation of LiFePO$_4$ battery is proposed in this work.
- The influence of battery hysteresis phenomena on the SOC estimation is analyzed.
- The impedance factor is utilized to take the battery aging effect into account.
- The estimation approach is verified with typical BEV and HEV current load cycles.
- Superior performance of SMC filtering compared to other approaches is shown.

ARTICLE INFO

ABSTRACT

Battery state monitoring is one of the key techniques in battery management systems e.g. in electric vehicles. An accurate estimation can help to improve the system performance and to prolong the battery remaining useful life. Main challenges for the state estimation for LiFePO$_4$ batteries are the flat characteristic of open-circuit-voltage over battery state of charge (SOC) and the existence of hysteresis phenomena. Classical estimation approaches like Kalman filtering show limitations to handle nonlinear and non-Gaussian error distribution problems. In addition, uncertainties in the battery model parameters must be taken into account to describe the battery degradation. In this paper, a novel model-based method combining a Sequential Monte Carlo filter with adaptive control to determine the cell SOC and its electric impedance is presented. The applicability of this dual estimator is verified using measurement data acquired from a commercial LiFePO$_4$ cell. Due to a better handling of the hysteresis problem, results show the benefits of the proposed method against the estimation with an Extended Kalman filter.

© 2013 Elsevier B.V. All rights reserved.

1. Introduction

Managing a battery pack of cells with LiFePO$_4$ (LFP) as cathode and graphite as anode material is a fundamentally challenging problem. Battery management systems (BMS) must be able to estimate the state of charge (SOC) and state of health (SOH) of the battery pack in order to prevent the battery from operating outside of its safety area and improve the battery performance with an optimal management strategy. However, these values cannot be measured directly. In addition, several factors make it difficult to realize an accurate estimation such as hysteresis phenomenon, flatness of open-circuit-voltage (OCV) over SOC and limited voltage measurement accuracy [1].

A classic approach to battery state estimation is Kalman filtering. Kalman filter (KF) algorithms containing a linear process and a linear measurement model are studied in Refs. [2,3]. Since the dynamics of electrochemical cells are not linear, two nonlinear extensions to the original KF were proposed, which are known as Extended Kalman filter (EKF) [4] and Unscented Kalman filter (UKF) [5]. EKF transforms the nonlinear system to a linear system by utilizing the first order Taylor series while the second approach approximates the system state by a small number of deterministically chosen samples. However, both methods operate with the assumption of Gaussian distribution, they suffer from an inherent inability to model the non-Gaussian probability density function (PDF) of the system states [6].

Moreover, a growing attention has been recently shown for the battery SOH indication since the battery storage system for automotive application is normally designed for ten years [7]. For system engineering, the battery aging is typically considered as

* Corresponding author. Tel.: +49 731 9530 537; fax: +49 731 9530 599.
  E-mail addresses: jiahao.li@zsw-bw.de, jiahao.li@gmx.de (J. Li).
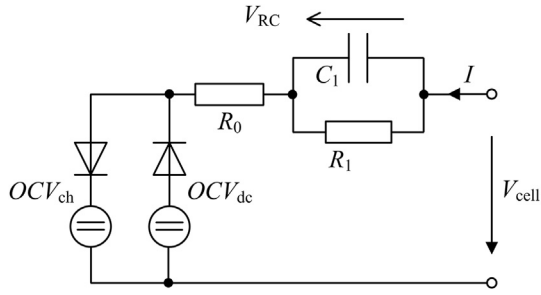
Fig. 1. Battery equivalent circuit model with open-circuit-voltage for charge OCV_{ch} and discharge OCV_{dc}, cell ohmic resistant R_0, resistance of RC-circuit R_1 as well as capacitance of RC-circuit C_1.

capacity fade and impedance rise. These effects should be taken into account in the estimation design.

This paper presents an estimation framework, where the battery SOC is estimated in the form of a PDF with an online adaption of its model parameters. First the influence of battery hysteresis on the state estimation is studied. After the introduction of the method, measurement data show its promising estimation performance with increased robustness in terms of battery aging process.

2. Battery modeling and OCV hysteresis effect

A battery equivalent circuit model commonly used for model-based state estimation design is shown in Fig. 1. The dynamic cell behavior is described by an impedance model which includes an ohmic resistance R_0 with a parallel branch of the resistor R_1 and the

capacitor C_1. In series to this element, two voltage sources provide the battery steady state cell behavior. They refer to the relaxed cell voltage after a charge or discharge process.

Based on the Coulomb counting law and the linear differential equation of an RC-circuit, the discrete-time dynamic equations of the cell model and the cell dynamic voltage can be expressed by

$$\begin{bmatrix} SOC_{k+1} \\ V_{RC,k+1} \end{bmatrix} = \begin{bmatrix} 1 & 0 \\ 0 & \frac{1-\Delta t}{R_1 C_1} \end{bmatrix} \cdot \begin{bmatrix} SOC_k \\ V_{RC,k} \end{bmatrix} + \begin{bmatrix} \eta_c \cdot \frac{\Delta t}{C_N} \\ \frac{\Delta t}{C_1} \end{bmatrix} \cdot I_k, \tag{1}$$

where k is the discrete-time index, Δt the sample time, V_{RC} the capacitor voltage, η_c the Coulombic efficiency, and C_N the discharge capacity of the battery. Thereby, the cell voltage is calculated according to Fig. 1 as

$$V_{cell,k} = OCV_{ch/dc}(SOC_k) + V_{RC,k} + R_0 \cdot I_k. \tag{2}$$

Considering the current I_k as the model input u_k, the state vector of the cell model can be chosen as

$$\mathbf{x}_k = \begin{bmatrix} SOC_k, V_{RC,k} \end{bmatrix}^T. \tag{3}$$

It is notable that the OCV value of an LFP cell differs from charge and discharge. Therefore this voltage uncertainty may result in poor BMS performance due to the fact that SOC estimation is based on the relationship between OCV and SOC [9].

In the following, Fig. 2 illustrates the influence of battery hysteresis phenomena on the state estimation. The idea is to determinate the battery SOC distribution from a Gaussian random variable with Monte Carlo sampling and EKF. The graph (a) shows the Monte Carlo method with 100 samples, which are generated

(a) (b) (c)
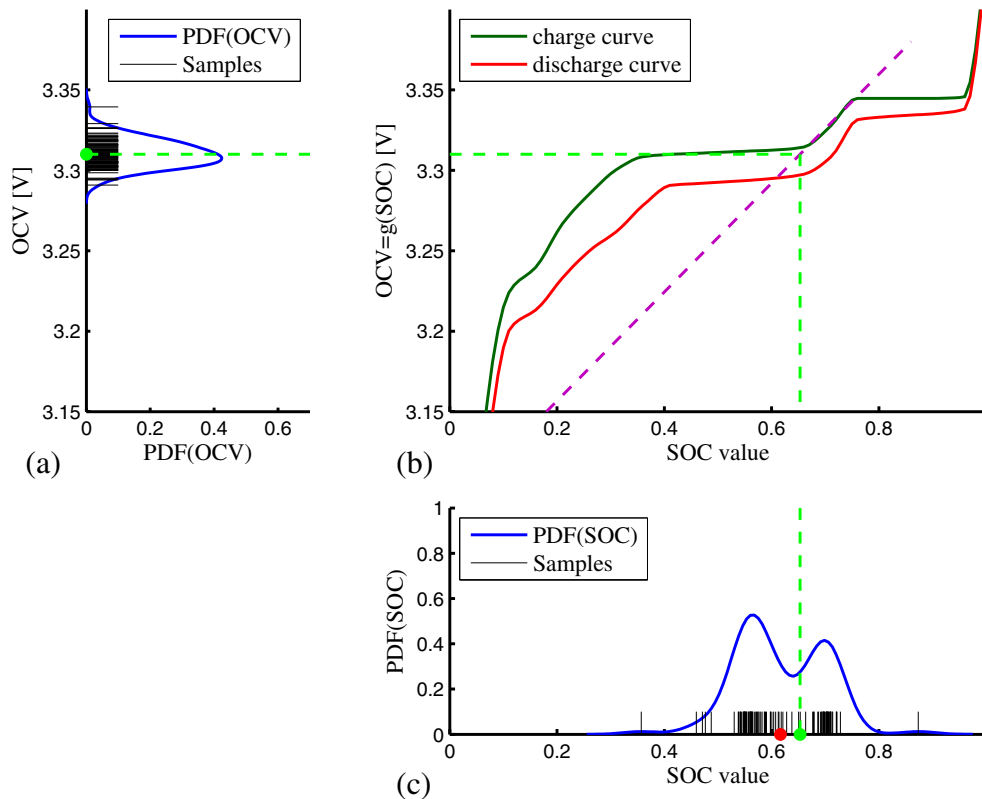
Fig. 2. Transformation of a Gaussian variable through OCV charge and discharge curve. (a) Gaussian random distribution of an OCV value. (b) Linear and nonlinear SOC−OCV transformation. (c) The resulting distribution of SOC samples. The red point shows the mean value of SOC distribution from Monte Carlo samples, whereas the green one is achieved by the EKF. (For interpretation of the references to color in this figure legend, the reader is referred to the web version of this article.)
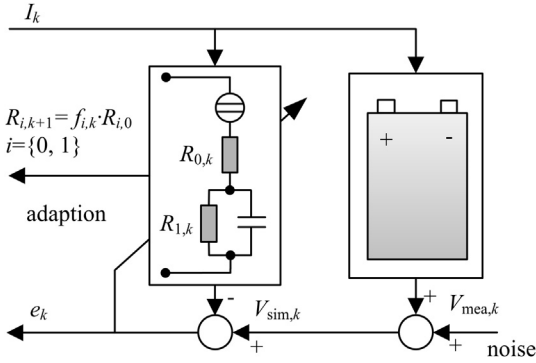
Fig. 3. Estimation of battery impedance factor through least mean squares (LMS) algorithm [16], with f_i the impedance factor, V_{sim} simulated and V_{mea} measured voltage.

from a Gaussian distribution with a mean value of 3.31 V. These samples are passed through the nonlinear SOC–OCV function (b). The resulting SOC samples are distributed in the graph (c) with their covariance, which correspond to a non-Gaussian distribution. The linearization curve (dashed in green), on the other hand, is achieved by the EKF. It approximates the SOC mean value by a linear function tangent to the OCV curve, retaining the Gaussian distribution of the system state. It can be clearly seen that Kalman based filtering tends to fail if the state distribution is non-Gaussian and has a bimodal PDF.

3. Battery parameter and state estimation

The estimation framework of the proposed system contains two main procedures, i.e. offline model initialization and online parameter tracking as well as SOC and SOH estimation.

3.1. Offline model initialization

Before the cell model is utilized for the onboard state estimation, the parameter vector $\theta = [R_0 R_1 C_1]$ from Fig. 1 must be initialized offline first. At a certain temperature, battery OCV can be measured and established by a nonlinear function or a lookup table. In comparison, the characterization of the impedance model is often provided by the current pulse measurement [10].

The parameterization tests carried out for this work are described in Ref. [11]. Since the behavior of lithium-ion batteries strongly depends on different states of the battery, the measurements including current pulses are done with different current direction, current rate at different SOC levels and ambient temperatures. Accordingly, the model's parameter vector $\theta = f(SOC,T,I)$ is a function of the battery's state variables. The parameters are identified using nonlinear least-squares methods, which minimize the error between the model output and experimental data until a predefined error criterion is satisfied.

3.2. Online impedance factor determination

Once the cell model is initialized, an online method is designed to track the battery aging effect during the load operation. Among the model parameters, the R_0 and R_1 show a significant change during the aging process [12]. Quasi linear increases in ohmic and charge transfer resistances of Li-ion cells over the energy throughput are observed [13,14]. The main idea of SOH monitoring in this work is to determine the impedance factors, reflecting the ratio between actual impedance and its initial value, to update the model parameters. It is known that different relaxation times of LFP

cells could be obtained using the electrochemical impedance spectroscopy (EIS) [20]. This phenomenon could not be simply reproduced by the battery model with a single RC-circuit. Through the online adaption of model parameters, the error performance of the presented model could be compensated at variant loads.

In comparison to tracking the absolute values, the impedance factor approach has the advantage to derive the relative changes of the model parameters at different temperatures without significant oscillations of the resistance values. Referring to the illustrated model (see Fig. 1), a least mean squares (LMS) filter is depicted in Fig. 3.

The voltage error

$$e_k = V_{mea,k} - V_{sim,k}, \tag{4}$$

which denotes the difference between the measured and simulated voltage, should be minimized:

$$\min_{\theta} \left[e_k e_k^T \right]. \tag{5}$$

Herein, the model elements are derived by

$$R_{0,k+1} = f_{0,k} \cdot R_{0,0}, \tag{6}$$

and

$$R_{1,k+1} = f_{1,k} \cdot R_{1,0}, \tag{7}$$

respectively under the assumption that the identified time constant will change during the aging process. $R_{0,0}$ and $R_{1,0}$ are the offline initialized impedance values. The prediction of model impedance proceeds on the basis of measurements. The filter will change the impedance factors $f_{i,k}$ in an attempt to reduce the voltage error. This update relation is expressed by

$$f_{i,k+1} = f_{i,k} + \mu_i \cdot I_k \cdot e_k, \text{ with } f_{i,0} = 1 \text{ and } i = \{0, 1\}, \tag{8}$$

where I_k is the battery current, μ_i is the step size of the adaptive filter. It is a tunable gain variable which controls the gradient term $\mu_i I_k e_k$ to update the coefficient. By increasing μ_i, the parameter adaption could be accelerated at the expense of the system stability and accuracy [8].

Compared to other adaptive filter algorithms such as the recursive least squares (RLS) algorithm described in Ref. [15], the LMS approaches do not involve any matrix operations. Thus, it requires fewer computational resources and memory, and simplifies the implementation on a microcontroller.

3.3. SMC filter based SOC determination

As mentioned before, the key idea underlying the SMC method, also known as particle filter, is to represent the system latent state by a set of randomly chosen samples with associated weights. As the number of samples becomes large, the Monte Carlo characterization approaches the optimal recursive Bayesian filter [6].
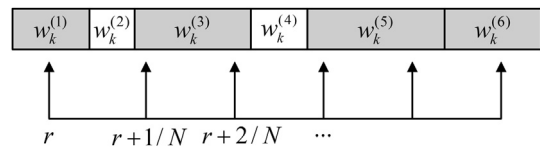

Fig. 4. Schematic diagram of the low variance resampling procedure [18].

In order to develop the details of the SMC algorithm, the state equations need to be modeled as a first order Markov chain with the outputs being conditionally independent at first. This is given by

$$\mathbf{x}_k = \mathbf{f}(\mathbf{x}_{k-1}, u_k) + \mathbf{n}_k, \quad \mathbf{x}(t_0) = \mathbf{x}_0, \tag{9}$$

and

$$z_k = g(\mathbf{x}_{k-1}, u_k) + v_k, \tag{10}$$

where $\mathbf{x}_k$, u_k and z_k are the system state, input and output. $\mathbf{f}(\ )$ and $g()$ are the nonlinear process model and the measurement model, $\mathbf{n}_k$ and v_k represent the system noise and the measurement noise. Both noise signals are treated as stochastic without any explicit assumption on the distribution form.

One commonly used technique for implementing a SMC filter is called sampling importance resampling (SIR) which combines the Sequential Importance Sampling (SIS) and the resampling step. It approximates the state distribution $p(\mathbf{x}_k|z_0, …, z_k)$ by a set of weighted particles denoted as

$$\left\{ \left(\mathbf{x}_k^{(i)}, w_k^{(i)} \right), \quad i = 1, …, N \right\}, \tag{11}$$

where $w_k^{(i)}$ are the importance weights which denote the relative state distribution of the samples. Furthermore, the expected state density and measurement value could be approximated as

$$E[p(\mathbf{x}_k|z_{1:k})] \approx \sum_i w_k^{(i)} \cdot \delta(\mathbf{x}_k - \mathbf{x}_k^{(i)}), \tag{12}$$

and

$$E[f(\mathbf{x}_k)|z_{1:k}] \approx \sum_i w_k^{(i)} \cdot f(\mathbf{x}_k^{(i)}). \tag{13}$$

For the battery SOC estimation, the SMC algorithm could be summarized as follows:

I. Initialization of the particles

At the beginning, new SOC particles are drawn from a known PDF, which could have a Gaussian or a uniform distribution around the feasible starting SOC point:

$$\mathbf{x}_0^{(i)} = \text{SOC}_0 + \pi\left(0, \sigma_0^2\right), \quad i = 1, …, N, \tag{14}$$

with variance σ_0^2.

II. Determination of the terminal voltages and the importance factors

In order to improve the SOC estimation accuracy, the hysteresis effect of LFP cells needs to be considered in the filtering design. In Fig. 2(c), a quasi bimodal Gaussian SOC distribution is obtained resulting from a normal distributed OCV value. In the following, the battery charge and discharge voltage is calculated respectively to cover the voltage possible distribution of the samples [17]:
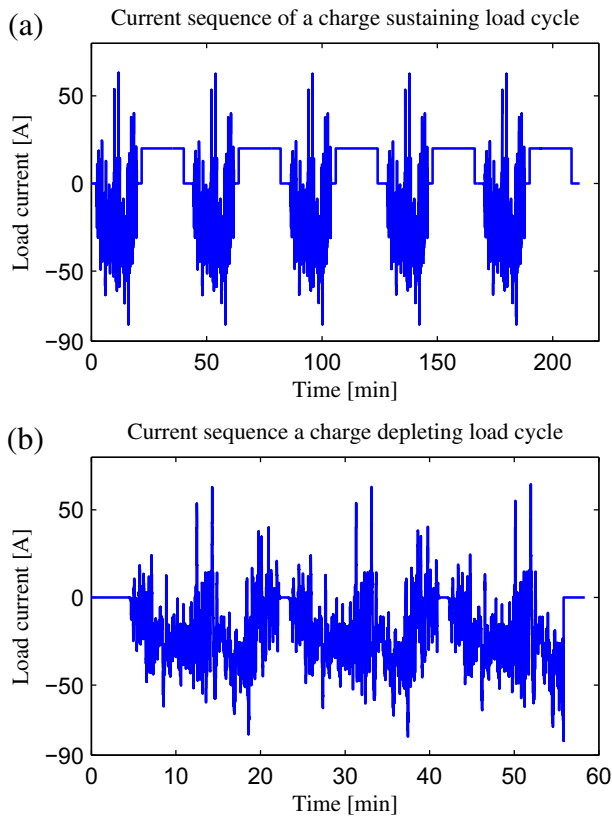

(a) Current sequence of a charge sustaining load cycle

(b) Current sequence a charge depleting load cycle

Fig. 5. Applied current sequences with ARTEMIS driving profiles for validating parameter and SOC estimations. (a) Charge sustaining load cycle with constant current charge procedures. (b) Charge depleting load cycle with ARTEMIS cycles in series.
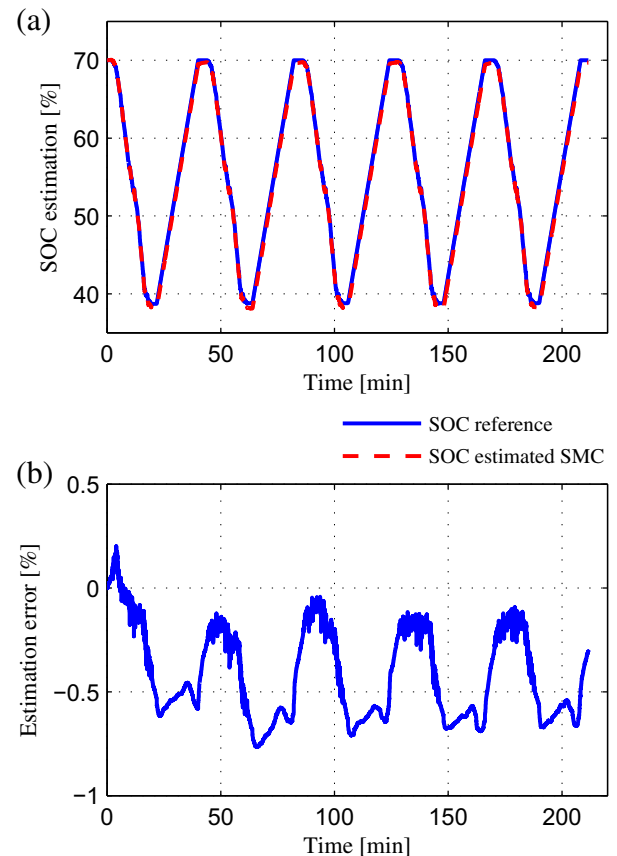

(a)

(b)

SOC reference
SOC estimated SMC

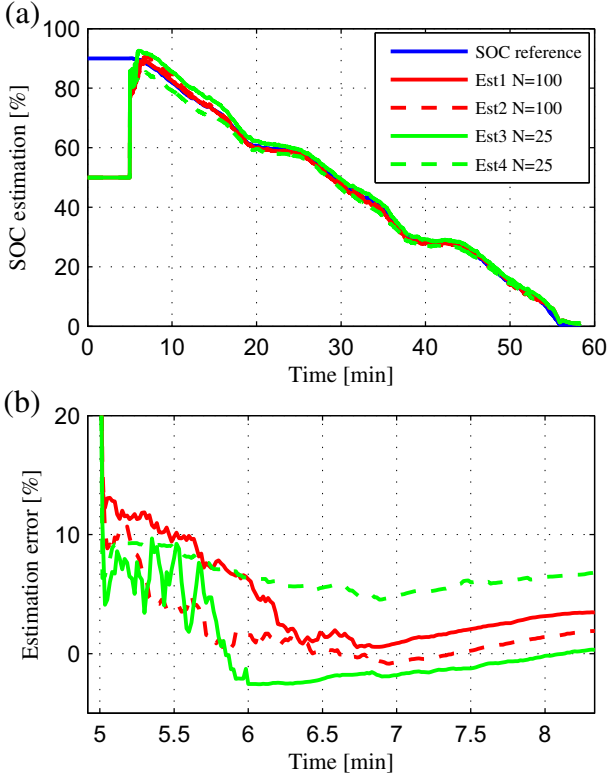**Fig. 6.** SOC behavior (a) and estimation error (b) under charge sustaining cycles.

Fig. 7. SOC behavior (a) and estimation error (b) with different sets of samples $N = 100$ and $N = 25$ for the entire cell operation range.

$$V_{\text{ch},k} = \text{OCV}_{\text{ch}}(\text{SOC}_k) + V_{\text{RC},k} + R_{0,k} \cdot I_k, \qquad (15)$$

and

$$V_{\text{dc},k} = \text{OCV}_{\text{dc}}(\text{SOC}_k) + V_{\text{RC},k} + R_{0,k} \cdot I_k. \qquad (16)$$

Hence, the probability of the measurement $V_{\text{mea},k}$ under the SOC particle SOC_k could be generated as the superposition of two individual weights, which are determined by two Gaussian distributions around V_{ch} and V_{dc} in

$$w_k^{(i)} = \frac{1}{\delta\sqrt{2\pi}} \cdot \left[\exp\left(-\frac{\left(V_{\text{ch},k}^{(i)} - V_{\text{mea},k}^{(i)}\right)}{2\delta^2} \right) \right. \\ \left. + \exp\left(-\frac{\left(V_{\text{dc},k}^{(i)} - V_{\text{mea},k}^{(i)}\right)}{2\delta^2} \right) \right], \qquad (17)$$

with variance δ^2. The weights are further normalized to one as follows:

$$w_k^{(i)} = \frac{w_k^{(i)}}{\sum_{i=1}^{N} w_k^{(i)}}. \qquad (18)$$

III. Resampling

The resampling process, also known as the importance sampling, is used in order to avoid the degeneracy problem of the samples [6]. In this step, samples with low importance weights are replaced by the samples with high importance weights. Several methods are introduced in Ref. [18] that might reduce the effect of

Table 1
Overview of estimation results with random sampling.

	25 Samples	100 Samples
RMSE	2.3%	1.4%
Convergence time (within 5% error)	76 s	42 s
Performance	Variable	Robust

degeneracy. In this work low variance sampling (LVS) strategy is executed, as described with the following Pseudocode:

The LVS algorithm involves a so-called sequential stochastic process. It computes a single random number at the beginning and then selects the particles by repeatedly adding a fixed amount value to this initial point. The particles that correspond to this resulting number will be chosen for the next step, which are displayed in gray in Fig. 4. Herewith, the probability of the selection is proportional to the sample weight.

IV. Estimation Output

The weighted values of the selected SOC particles are recursively summed up to

$$\widehat{\mathbf{x}}_k = \sum_{i=1}^{N} w_k^{(i)} \cdot \mathbf{x}_k^{(i)}, \qquad (19)$$

which is considered to be the estimation result for each iteration.

4. Experimental details

In order to validate the presented parameter and SOC estimation algorithms, load tests are carried out with a commercial LFP pouch cell, having a nominal capacity of 20 Ah and a nominal voltage of 3.3 V.

Two current profiles, derived from the ARTEMIS driving cycle [19], are applied and depicted in Fig. 5 (normalized to a cell's nominal capacity). The first test is a sequence of ARTEMIS current profiles followed by a constant charge phase (10 min rest between two cycles). This test is designed to evaluate the estimation performance under both the dynamic and static loads. The used load current cycle is charge neutral, which is a typical load profile of a hybrid electric vehicle (HEV). In the second test, the entire operating range of the cell is utilized (typical load of an electric vehicle). The ARTEMIS load cycle, started with 90% SOC, is repeated until the cell voltage reaches its limitation.

The tests are done on a BaSyTec HPS test bench (0–10 V, ±250 A). The accuracy of both voltage and current measurement is within 0.05 % of the full scale range, and the resolution within 0.003%. During the test, the cell is placed in a climatic chamber ESPEC PU-3KP (temperature range −40 °C to +100 °C, accuracy: ±0.5 °C) and the cell ambient temperature is constantly held at 30 °C. Data points are collected at 50 Hz during the tests. For the validation test, the value from the current integration serves as the actual SOC behavior.

5. Results and discussion

5.1. Current profile of a charge sustaining load cycle

Results using SMC filter to estimate SOC for the first test regime is shown in Fig. 6, where the cell SOC is cycled between 70% and 40%. The SOC is correctly initialized to 70%, and the estimation error starts from zero. Generally, the estimated SOC behavior is consistent with the reference and the deviation is hardly visible. As can be seen in the graph, at first the error diverges slowly away from the true SOC behavior during the discharge portion and then
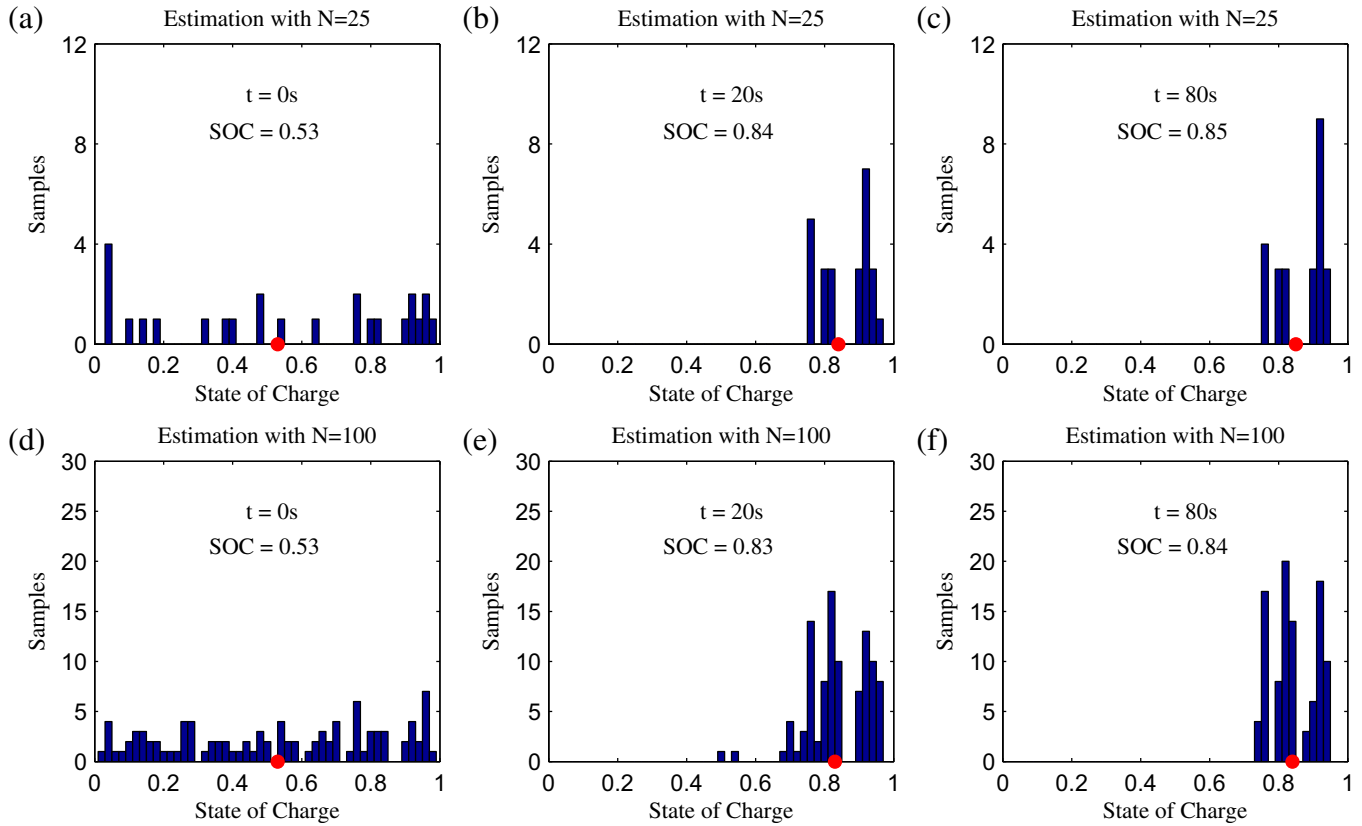
Fig. 8. Mean values and the variance of two sets of SOC samples at different simulation time points.

repeatedly converges at the charge segment. One possible reason is that the cell SOC–OCV curve shows an extreme flat relationship in this region (see Fig. 2(b)), so that the estimation accuracy might be influenced by the voltage measurement and Coulombic counting error.

5.2. Current profile of a load cycle with whole SOC range

In this section, ARTEMIS current profiles are loaded in series to evaluate the estimation performance for the entire cell operation
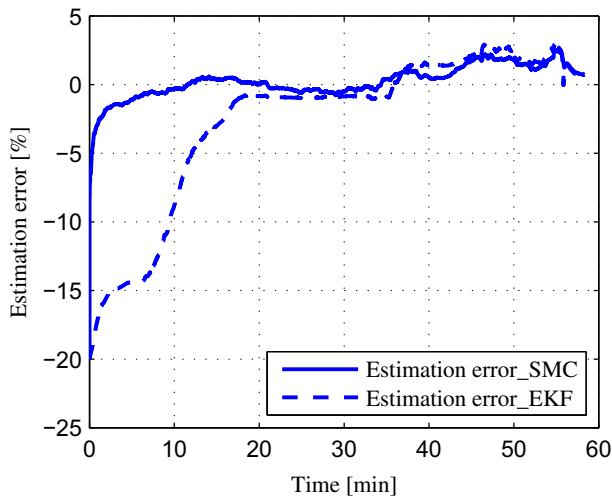

Fig. 9. Comparison of the estimation error between SMC and EKF under ARTEMIS with 20% start SOC error.

range. Fig. 7 depicts the estimation results with an unobservable start SOC. Note that the battery SOC estimator is activated after 5 min, when the current load occurs.

The simulations with two sets of samples (twice with 100, twice with 25) are run for four times. Due to the Monte Carlo random sampling method, the non-deterministic behavior of particle filter is shown. Obviously, the estimation trajectories with 100 samples are more consistent to each other, whereas the variance of 25 samples is comparatively higher. An overview of the estimation results in terms of root mean square error (RMSE) and convergence rate is presented in Table 1. In addition, Fig. 8 illustrates a histogram about the distribution of the particles at three estimation time points.

At the beginning, all samples are spread throughout the state space from 0 to 100%. After that, they are converging to the real SOC value. Because of the hysteresis modeling with two Gaussian functions (17), a bimodal SOC distribution could be obtained from both simulations. The estimated SOC is calculated as the weighted value in (19).

5.3. Comparison of estimation with SMC and EKF

The achieved SOC performance with SMC is subsequently compared to the estimation with EKF previously described in Ref. [1] (Section 5). Simulations are carried out with the same ARTEMIS drive profile starting from 90% initial SOC as in Fig. 7. All experimental data used are identical. The estimation error is plotted in Fig. 9, where both filters are incorrectly initialized to SOC = 70%.

It is notable that the estimation error from EKF is identical to the one in Ref. [1] and is replicated here to compare with the SMC result. The EKF has an RMSE of 6.2%, while the SMC with 100 samples has an RMSE of 1.42%. In this case the advantageous
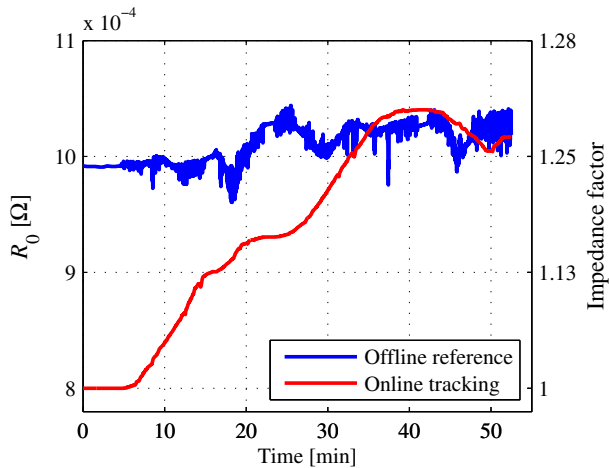
Fig. 10. Adaption of the impedance factor and the ohmic resistance with incorrect initial value.

performance of SMC can be clearly seen. Due to the reconstruction of the nonlinear process with the PDF rather than local linearization, the SMC filter enables a much faster convergence rate and a more accurate estimation result.

5.4. Adaption of model parameters

To evaluate the algorithm of online parameter identification, the model parameters are initialized with incorrect values (approx. 20% start error). As an example, a tracking result of the impedance factor of the ohmic resistance is shown in Fig. 10. Simulation is carried out with the same current profile as in Section 5.2. Since the cell real resistance cannot be directly measured, the value from the lookup table of the offline model serves as the reference behavior. As the current flows, the estimated resistance converges in the direction to its real value till the end of the simulation. Note that the correction applied to the impedance factor depends on the voltage error and the coefficient μ_i in (8). In the real application, this correction term is usually selected as a small value to improve the robustness of the filter.

6. Conclusion

To summarize, a novel framework of state estimation for LiFePO$_4$ battery combining Sequential Monte Carlo and adaptive filtering is proposed in this work. In comparison with the traditional Kalman filtering, where the PDF could be reconstructed by means of means and covariance, the SMC approach uses a set of weighted samples to approximate the state distribution of a nonlinear, non-Gaussian battery model. In practice, if enough samples are chosen, the observation could be very close to the true value [18]. The advantages of a SMC filter for battery state estimation could be concluded as:

- SMC algorithm reduces the requirements of modeling accuracy. The hysteresis effect of LFP cell could be modeled by a bi-Gaussian distribution.
- SMC-based framework allows to compute the PDF of estimated SOC values.

- The superior performance is reflected in the convergence rate with an unobservable start SOC.

Moreover, the battery SOH is considered as the impedance rise in this work. Based on the voltage deviation between measurement and battery model, an adaptive observer with the LMS method is developed to update the model parameters in the online estimation. Instead of tracking the absolute model values, the impedance factor approach has the advantage to deal with the parameter uncertainty under different operation conditions. Combined with SMC algorithm, this model-based estimation framework enables an accurate and robust BMS application.

References

[1] J. Li, J.K. Barillas, C. Guenther, M.A. Danzer, J. Power Sources 230 (2013) 244–250.
[2] J. Wang, J. Guo, L. Ding, Energy Convers. Manage. (2009) 3182–3186.
[3] P. Spagmpö, S. Rossi, S.M. Savaresi, in: IEEE Control Applications (CCA), 2011, pp. 587–592.
[4] Gregory L. Plett, J. Power Sources 134 (2004) 277–292.
[5] Gregory L. Plett, J. Power Sources 161 (2006) 1356–1368.
[6] B. Ristic, S. Arulampalam, N. Gordon, Beyond the Kalman Filter, The Artech House Press, USA, 2006.
[7] Y. Chiang, W. Sean, J. Ke, J. Power Sources 196 (2011) 3921–3932.
[8] M. Roscher, O. Bohlen, D. Sauer, IEEE Trans. Energy Convers. 3 (2011) 737–743.
[9] J. Kim, G. Seo, in: IEEE Electric Vehicle Conference, 2012, pp. 1–5.
[10] R. Benger, H. Wenzl, H. Beck, M. Jiang, D. Ohms, G. Schaedlich, World Electr. Veh. J. 3 (2009).
[11] C. Guenther, J. Barillas, S. Stumpp, M. Danzer, in: IEEE 3rd ISGT Europe, 2012.
[12] Z. Bing, X. Wie, in: IEEE 9th ICMTMA, 2009, pp. 388–392.
[13] M. Broussely, Ph. Biensan, F. Bonhomme, Ph. Blanchard, S. Herreyre, K. Nechev, R.J. Staniewicz, J. Power Sources 146 (2005) 90–96.
[14] U. Tröltzsch, O. Kanoun, H. Tränkler, Electrochim. Acta 51 (2006) 1664–1672.
[15] X. Hu, F. Sun, Y. Zou, H. Peng, in: IEEE American Control Conference, 2011, pp. 935–940.
[16] A. Jossen, W. Weydanz, Moderne Akkumulatoren Richtig Einsetzen, Inge Reichardt Press, 2006.
[17] S. Schwunk, N. Armbruster, S. Straub, J. Kehl, M. Vetter, J. Power Sources 239 (2013) 705–710.
[18] S. Thrun, W. Brgard, D. Fox, Probabilistic Robotic, The MIT Press, 2006.
[19] M. Andre, J. Power Sources 334 (2004) 73–84.
[20] J. Schmidt, T. Chrobak, M. Ender, J. Illig, D. Klotz, E. Ivers-Tiffée, J. Power Sources 196 (2011) 5342–5348.

Nomenclature

C_1: equivalent circuit capacitance (F)
C_N: cell discharge capacity (Ah)
e: voltage error between the measured and simulated voltage (V)
$\boldsymbol{f}$: system vector of cell equivalent circuit model
f: cell impedance factor
g: output function of cell equivalent circuit model
I: cell charge or discharge current (A)
k: discrete time index
$\boldsymbol{n}$: stochastic system noise
OCV_{ch}: open-circuit-voltage after charging (V)
OCV_{dc}: open-circuit-voltage after discharging (V)
p: distribution of the system states
R_0: cell ohmic resistance (Ω)
R_1: equivalent circuit resistance (Ω)
SOC: battery state of charge
T: cell temperature (°C)
u: input vector of cell equivalent circuit model
V_{RC}: capacitor voltage (V)
v: stochastic measurement noise
w: Importance weight of the samples
$\boldsymbol{x}$: state vector of cell equivalent circuit model
z: output of cell equivalent circuit model
μ: step size of the adaptive filter
η_c: Coulombic efficiency
σ: variance
$\boldsymbol{\theta}$: vector of model parameters